



# Ethane measurement by Picarro CRDS G2201-i in laboratory and field conditions: potential and limitations

Sara M. Defratyka<sup>1</sup>, Jean-Daniel Paris<sup>1</sup>, Camille Yver-Kwok<sup>1</sup>, Daniel Loeb<sup>1, \*</sup>, James France<sup>2, 3</sup>, Jon Helmore<sup>4</sup>, Nigel Yarrow<sup>4</sup>, Valérie Gros<sup>1</sup>, Philippe Bousquet<sup>1</sup>

5 1 Laboratoire des sciences du climat et de l'environnement (LSCE-IPSL) CEA-CNRS-UVSQ Université Paris Saclay, Gif-sur-Yvette, 91191, France

2 Royal Holloway University of London, Egham, TW20 0EX, United Kingdom

3 British Antarctic Survey, Natural Environment Research Council, Cambridge CB3 0ET, UK

4 National Physical Laboratory (NPL), Hampton Road, Teddington, TW11 0LW Middlesex, UK

10 \*Now at Université Paris-Saclay, Orsay 91400

*Correspondence to:* Sara M. Defratyka (sara.defratyka@lsce.ipsl.fr)

**Abstract** Ethane can be used as a tracer gas to distinguish methane sources, both at the local and global scale. Currently, ethane can be successfully measured using flasks or dedicated in-situ analyzers. In our study, we consider the possibility of using the CRDS Picarro G2201-i instrument, dedicated to isotopic CH<sub>4</sub> and CO<sub>2</sub>, for suitable measurements of ethane:methane ratio in mobile field, near-source conditions. Our work was divided into three steps. First, laboratory tests were run to characterize the instrument in stationary conditions. Then the instrument performance was tested in the field, as part of a controlled release experiment and finally during mobile measurements focused on gas compressor stations. The results from the field are compared with the results from other instruments, dedicated to ethane measurements. Our study clearly shows the potential of using the CRDS G2201-i instrument to determine the ethane:methane ratio in methane plumes in mobile condition with an ethane uncertainty of 50 ppb. Assuming typical ethane to methane ratio ranging between 0 and 0.1 ppb ppb<sup>-1</sup> we conclude that the instrument can correctly estimate the “true” ethane to methane ratio within 1-sigma uncertainty in CH<sub>4</sub> enhancements of 1 ppm or more as can be found in the vicinity of strongly emitting sites (such as natural gas compressor station).

## 1. Introduction

Methane (CH<sub>4</sub>) is the second most potent anthropogenic greenhouse gas, and its global average mixing ratio reached 1.876 ppm in the atmosphere in March 2020 (Dlugokencky, 2020), approximately three times more than during the pre-industrial era. Anthropogenic methane emissions amount to half of the total input of methane to the atmosphere and include a range of sources such as landfill, wastewater treatment plants, agriculture, coal, oil, and natural gas industries (IPCC, 2018; Turner et al., 2019; Saunio et al., 2020). Large uncertainties remain in the quantification of these sources magnitudes and locations (Saunio et al., 2016). The variety of methane sources and their geographical overlap increase the difficulty of closing the present methane budget from global to local scales.



Some methane sources also co-emit other gases that can be used as tracers to identify them. For instance, ethane ( $C_2H_6$ ) is associated with thermogenic methane and it is therefore co-emitted during extraction of coal, oil and natural gas as well as transportation of the latter (e.g., Aydin et al., 2011; Hausmann et al., 2016; Helmig et al., 2016; Schwietzke et al., 2014; Sherwood et al., 2017; Simpson et al., 2012). In the case of the natural gas industry, a range of values for ethane:methane ( $C_2H_6:CH_4$ ) ratio are observed according to the geological reservoir from which the gas has been extracted and by its eventual processing. The reported ratios depend on the type of facilities and type of the reservoirs: between 0.01 and 0.06 for gas leaks and gas compressors (Lopez et al., 2017; Lowry et al., 2020; Yacovitch et al., 2014), or higher than 0.3 for processed natural gas liquids (Kort et al., 2016; Yacovitch et al., 2014). Also, different ratios are observed in the case of dry gas (0.01-0.06) and wet gas ( $>0.06$ ). In the case of offshore oil and gas platforms,  $C_2H_6:CH_4$  ratios typically were around 0.05, but ratios equal to 0.002 and 0.17 were observed as well (Yacovitch et al., 2020). On the contrary, biogenic sources such as landfills and cattle farms show null to very small  $C_2H_6:CH_4$  ratio ( $<0.002$ ) (Assan et al., 2017; Yacovitch et al., 2014).

At the local scale, observing changes in  $C_2H_6:CH_4$  ratio provides additional information about specific methane enhancement source, especially in areas with multiple  $CH_4$  enhancements from unknown origins (Assan et al., 2017; Lopez et al., 2017; Lowry et al., 2020; Yacovitch et al., 2014, 2020). The currently available techniques, such as Gas Chromatography with Flame Ionization Detector (GC-FID) and Fourier-Transform Infrared Spectroscopy (FTIR) provide access to long-term or short-term measurements of ethane and other components in stationary conditions (Bourtsoukidis et al., 2019; Gros et al., 2011; Hausmann et al., 2016; McKain et al., 2015; Yang et al., 2005). Additionally, laser-based instruments, such as the Los Gatos Research (LGR) Ultraportable Methane:Ethane Analyzer (UMEA), based on a cavity-enhanced absorption technique, the Picarro Cavity Ring Down Spectroscopy (CRDS) analyzers (Rella et al. 2015) and the tunable infrared laser direct absorption spectroscopy (TILDAS) analyzer (Smith et al., 2015; Yacovitch et al., 2014) make it possible to perform measurements of ethane using a mobile platform.

Previous studies already showed the possibility of using a laser based cavity instrument to determine the  $C_2H_6:CH_4$  ratio (Rella et al. 2015; Assan et al. 2017; Lopez et al. 2017, Lowry et al. 2020). In the study of Assan et al. (2017), a CRDS G2201-i dedicated to the measure of  $^{12}CO_2$ ,  $^{13}CO_2$ ,  $^{12}CH_4$ ,  $^{13}CH_4$  and  $H_2O$  was located stationary nearby natural gas facilities. Over two weeks, dried ambient air was measured simultaneously by CRDS G2201-i and GC-FID, using the 10-minute averages for 16 “events” of high methane mixing ratios lasting more than 1 hour. The  $C_2H_6:CH_4$  ratio separated events of biogenic or thermogenic origin. Moreover, during that study, flask samples were collected and further analyzed in the laboratory. The laboratory values showed good agreement between field CRDS G2201-i and GC-FID results (Assan et al. 2017).

Rella et al. (2015) and Lopez et al. (2017) used the CRDS instrument as part of a mobile setup enhanced with a storage tube, called AirCore (Karion et al. 2010). This storage tube allows to improve time resolution and hence precision. The mobile measurements can be made in two modes using this setup. During the “monitoring mode” the air is split and injected at the same time directly to the instrument and to the AirCore. In the “replay mode”, air from the AirCore is measured. Using the AirCore with a lower flow rate increases the sampling frequency. The replay mode is only used after observation of a methane plume (Rella et al. 2015; Lopez et al. 2017; Hoheisel et al. 2019). In the study by Lopez et al. (2017),  $C_2H_6:CH_4$  ratios were



65 estimated for natural gas facilities. For gas pipelines, the CRDS G2201-i results were compared with results obtained from  
flask measurements analyzed by gas chromatography. The results showed good agreement between the two methods (Lopez  
et al. 2017).

Here, the main purpose of this study is to evaluate the performance of the CRDS G2201-i and the applicability of making  
short-term, direct, continuous, mobile measurements of ethane in methane-enriched air, with sufficient precision during near  
70 source (“pollution plume conditions”) surveys. To achieve this goal, following Assan et al. (2017), the first step consists of  
laboratory tests to calculate the calibration factors and also to check the instrument performance in stationary, laboratory  
conditions. The second step is to investigate the performance of the instrument during field measurements. A tracer release  
experiment was performed where a methane and ethane mixture with known C<sub>2</sub>:C<sub>1</sub> ratio and emission flux was emitted and  
compared to measured ratios from CRDS G2201-i and LGR UMEA. Thirdly, the instrument has also been evaluated in real  
75 field conditions, during surveys conducted at gas compressor stations and one landfill. In this step, measured values are  
compared to values from gas chromatography and those provided by the owner of the gas compressor stations. These extensive  
and complex tests allow for a full characterization of the CRDS G2201-i instrument to ethane measurements and provide  
broader knowledge about the limitations of this instrument when measuring C<sub>2</sub>H<sub>6</sub>:CH<sub>4</sub> ratios.

Subsequently, after presenting material and methods for these three steps (section 2), their results are presented (section 3) and  
80 discussed (section 4).

## 2. Material and Methods:

The CRDS G2201-i (Picarro Inc., Santa Clara USA), used during this study, is dedicated to the measurements of the mixing  
ratio of <sup>12</sup>C<sup>16</sup>O<sub>2</sub>, <sup>13</sup>C<sup>16</sup>O<sub>2</sub>, <sup>12</sup>C<sup>1</sup>H<sub>4</sub>, <sup>13</sup>C<sup>1</sup>H<sub>4</sub> and <sup>1</sup>H<sub>2</sub><sup>16</sup>O (further H<sub>2</sub>O). It operates in three spectral lines: 6057, 6251 and 6029 cm<sup>-1</sup>.  
As there is an interference of <sup>12</sup>C<sub>2</sub><sup>1</sup>H<sub>6</sub> (further C<sub>2</sub>H<sub>6</sub>) on <sup>13</sup>CH<sub>4</sub> in the absorption spectra, this instrument also measures C<sub>2</sub>H<sub>6</sub>  
85 to correct this interference. Due to observed interferences with <sup>12</sup>C<sup>16</sup>O<sub>2</sub> (further CO<sub>2</sub>), H<sub>2</sub>O and <sup>12</sup>CH<sub>4</sub>, measured C<sub>2</sub>H<sub>6</sub> values  
must be first corrected. The study performed by Assan et al. (2017) provided the strategy to determine the factors to correct  
the measured C<sub>2</sub>H<sub>6</sub> mixing ratio due to the interference with other species:

$$\text{C}_2\text{H}_6 \text{ corrected} = \text{C}_2\text{H}_6 \text{ raw} + \text{A} \cdot \text{H}_2\text{O} + \text{B} \cdot \text{CH}_4 + \text{C} \cdot \text{CO}_2 \quad (1).$$

Based on their tests, the interference of other species on C<sub>2</sub>H<sub>6</sub> changes in relation to the water vapor level in the measured  
90 sample. The correction factors were determined for two different CRDS G2201-i devices (CFIDS 2067 and CFIDS 2072) (see  
Assan et al. 2017). According to that study, if the water vapor level in the measured gas is less than 0.16% (“low humidity  
case”), then interference correction factors are the same for both devices. In the presence of water vapor (=>0.16%, “high  
humidity case”), the correction factors were different for each device. The threshold of 0.16% corresponds to 26.14% of  
relative humidity in standard conditions of temperature and pressure. Due to these differences, drying air is strongly  
95 recommended before making measurements (Assan et al. 2017). In the study presented in this article, the correction factors,  
determined by Assan et al. (2017) are used.



Ethane measured by the G2201-i must eventually be linked to a widely used scale, to ensure comparability and traceability. Finally, corrected and calibrated C<sub>2</sub>H<sub>6</sub> values can be used to determine the C<sub>2</sub>H<sub>6</sub> correction on δ<sup>13</sup>CH<sub>4</sub> mixing ratio or, as in this study, to determine the ethane to methane ratio. Here, the same device (CRDS G2201-i CFIDS 2072) was used as by  
100 Assan et al. (2017); which allows checking possible long-time drift in previously-calculated calibration factors. As outlined in the introduction, three different setups were used to test the instrument capability: laboratory, controlled-release experiment, and field experiment.

## 2.1. Laboratory setup

We conducted four different tests: the first one to determine the calibration factors, then the others to evaluate the instrument  
105 continuous measurement repeatability (CMR, commonly known as precision), Allan variance, time drift and water vapor sensitivity (Allan, 1966; Yver Kwok et al., 2015).

Here, the calibration factors are calculated using the approach presented by Hoheisel (2018), where a synthetic gas mixture of known C<sub>2</sub>H<sub>6</sub> (“target”), is diluted with a dilution gas with known CO<sub>2</sub> and CH<sub>4</sub> mixing ratios and applying the following equation:

$$110 \quad C_2H_6 \text{ true} = \left( 1 - \frac{1}{2} \left( \frac{CH_4 \text{ meas}}{CH_4 \text{ dilution}} + \frac{CO_2 \text{ meas}}{CO_2 \text{ dilution}} \right) \right) \cdot C_2H_6 \text{ target} \quad (2).$$

where C<sub>2</sub>H<sub>6 true</sub> is the ethane mole fraction obtained by mixing air from two cylinders, one containing ethane at a known value (C<sub>2</sub>H<sub>6 target</sub>) (without presence of methane or carbon dioxide) and one without ethane but with typical ambient mole fraction methane and carbon dioxide mixing ratio (dilution gas) using a mass flow controller (MFC). CH<sub>4 dilution</sub> and CO<sub>2 dilution</sub> are the  
115 mixing ratio of the dilution gas. CH<sub>4 meas</sub> CO<sub>2 meas</sub> are average measured mixing ratios after dilution. This calculation is repeated for different C<sub>2</sub>H<sub>6</sub>:CH<sub>4</sub> ratios, determined using the MFCs. The calibration factors are calculated as the slope and intercept of the linear regression of measured C<sub>2</sub>H<sub>6</sub> versus true C<sub>2</sub>H<sub>6</sub>.

The calculation of the calibration factors is implemented through a linearity test, where the C<sub>2</sub>H<sub>6</sub>:CH<sub>4</sub> ratio is gradually increased from 0.00 to 0.15 and measured for 20 minutes for each step. This measurement cycle is repeated three times. To do so, based on the setup presented by Assan et al. (2017), a working gas with ethane mixing ratio ~50 ppm is mixed with the  
120 dilution gas via two mass flow controllers. As the flow rate of the measured gas is greater than the instrument’s inlet allowance, an open split is installed before the analyzer to vent the generated mixture and maintain an ambient pressure at the instrument inlet. This test was repeated twice: in January 2018 and April 2019. The central 15 minutes of each 20-minute measurements are kept for further analysis. Then, the calibration factors are calculated as a regression slope and an intercept of the linear fitting, of theoretical (Eq. 2) against measured C<sub>2</sub>H<sub>6</sub> with already applied correction factors from Equations 1.

125 The CMR test has been made by measuring a working gas continuously over 24 hours and CMR is calculated as the one standard deviation (SD) over different averaging times (see Yver Kwok et al., 2015). This test was made twice: first using a working gas with negligible amount of ethane and the second time with a gas mixture where C<sub>2</sub>H<sub>6</sub>:CH<sub>4</sub> ratio was equal to 0.05. This test helps to determine the CMR and instrument noise in the absence or presence of ethane. Moreover, the Allan deviation



is also calculated to determine the noise response of the instrument over different averaging times. Typically, the Allan  
130 deviation decreases for increasing averaging time. However, depending on the instrument, with increasing of averaging time,  
the instrument drift can contribute to the increase of the Allan deviation. Thus, the optimal averaging time can be identified  
(Allan, 1966).

Also, another target gas, traceable to the WMO X2004A CH<sub>4</sub> scale, has been measured during 20 minutes, with a CH<sub>4</sub> mixing  
ratio about 10 000 ppb and a C<sub>2</sub>H<sub>6</sub> mixing ratio about 1 000 ppb. The CH<sub>4</sub> mixing ratio was measured with a CMR of about  
135 1 ppb, while for C<sub>2</sub>H<sub>6</sub> the CMR of the measurement was about 50 ppb (Section 3.1). This test allows us to determine the  
linearity and short-time precision of the instrument for a gas with a higher mixing ratio than that of ambient air, both of C<sub>2</sub>H<sub>6</sub>  
and CH<sub>4</sub>.

The drift of the C<sub>2</sub>H<sub>6</sub> baseline between December 2018 and May 2019 has also been investigated. The known working gas  
(dry atmospheric mixing ratio of CH<sub>4</sub> with negligible C<sub>2</sub>H<sub>6</sub>) was measured during 11 randomly chosen days, 20 times over  
140 that period, about 20 minutes each time. That measurement was made systematically as part of the mobile-measurement  
protocol (described below). The gas was measured before and after surveys to check instrument stability and influence of  
switching it on and off.

We finally ran a water vapor sensitivity test to revise the parameters of the correction (Eq. 1) in wet air. The target gas had a  
negligible C<sub>2</sub>H<sub>6</sub> mixing ratio. During the test, the target gas was progressively humidified (0 to 3 %) by steps of 0.25%, using  
145 a liquid flow controller (Liquiflow, Bronkhorst, Ruurlu, the Netherlands) and MFC coupled to a controlled evaporator mixer  
(CME). Each step lasted 20 minutes. The cycle was repeated three times. During data analysis, the interference correction  
factors determined by Assan et al. (2017) were applied. Three cases were tested: no interference correction (“Protocol 1”),  
high humidity case (“Protocol 2”) and low humidity case (“Protocol 3”) (excepted for the first step with dry air, where only  
the low humidity correction was applied).

## 150 2.2. Controlled-release experiment setup

This section describes the car-based instrument set-up in a controlled gas release experiment. The measurement set-up used  
here is the same as in the field (Section 2.4). The general principle of the setup is comparable to the previous works (e.g.,  
Hoheisel et al., 2019; Lopez et al., 2017; Rella et al., 2015). As the instrument is not dedicated to C<sub>2</sub>H<sub>6</sub> measurements, the  
vibrations induced by the motion of the car cause noise in the instrument readouts. Such a constraint can be overcome using  
155 two approaches. First, by stopping the car and standing some time inside the plume. Second, by accumulating air in the AirCore  
(Karion et al. 2010; Rella et al. 2015; Lopez et al. 2017) while moving through the plume and eventually reinjecting the  
AirCore’s air into the analyzer while stopped. Previously, the AirCore tool was successfully used as part of a mobile  
measurement setup to determine the isotopic composition of the methane source (Rella et al. 2015; Hoheisel et al. 2019; Lopez  
et al. 2017) and to determine C<sub>2</sub>H<sub>6</sub>:CH<sub>4</sub> ratio (Lopez et al. 2017).



160 For all mobile measurements, the background mixing ratios are calculated as the 1<sup>st</sup> percentile of the data sampled just before and just after the plumes, both for CH<sub>4</sub> and C<sub>2</sub>H<sub>6</sub>. Then the data with CH<sub>4</sub> enhancements above background are further analyzed. The C<sub>2</sub>H<sub>6</sub>:CH<sub>4</sub> ratio is calculated for each release as the slope of the linear regression of C<sub>2</sub>H<sub>6</sub> against CH<sub>4</sub>.  
In September 2019, during five days, a gas release experiment was conducted by the National Physical Laboratory (NPL, UK) and the Royal Holloway University of London (RHUL, UK). The experiment took place in Bedford Aerodrome, UK. The  
165 description of experimental setup configuration can be find in Gardiner et al. (2017) The goal was to evaluate the methods for calculating C<sub>2</sub>H<sub>6</sub>:CH<sub>4</sub> ratios, emission flux and isotopic composition during local mobile measurements. Each release lasted about 45 minutes. During the experiment, the parameters of each release: C<sub>2</sub>H<sub>6</sub>:CH<sub>4</sub> ratio (0.00 to 0.07), emission flux (until 70 L/min) and the source height (ground or ~4 m source) could vary. Here, results from 10 releases with known parameters and varying ethane:methane ratios are presented.

170 Seven releases were measured using the mobile setup (AirCore and standing in the plume). Air was dried before entering the analyzer using a magnesium perchlorate cartridge. Due to the limited time of the releases, the time of standing inside the peaks field was in the range of 15 to 20 minutes. After correcting raw data according to Eq. (1), following Protocol 3 (low humidity case), the calibration factors (section 2.1) are applied for the trace release and field work datasets.

Three other releases were measured using sampling bags (5 liters' skc flexfoil sample bags) only. Between 1 and 3 bags  
175 sampled inside the plume and one sampled outside as a background sample. Afterward, bags samples were measured in the laboratory using the CRDS G2201-i. The samples were measured without drying and the correction was applied for water vapor higher than 0.16% (Protocol 2). Then the C<sub>2</sub>H<sub>6</sub>:CH<sub>4</sub> enhancement ratio was calculated for every bag separately and also as a regression slope of C<sub>2</sub>H<sub>6</sub> against CH<sub>4</sub> values.

### 2.3. Field experiment setup

180 As a final step to evaluate G2201-i performance in mobile, real field conditions, the mobile-measurement set-up, described in Sect. 2.2 has been used during surveys made in the Paris area (see Defratyka et al., 2020, submitted). During spring and summer 2019, 6 surveys focused on three gas compressor stations (one survey for one of them and two surveys for the other two) and one landfill (one survey). All measurements were made outside of the sites, from the closest public road. To measure C<sub>2</sub>H<sub>6</sub>:CH<sub>4</sub> ratio, the car was stopped inside the plumes for about 35 minutes, and the central 30 minutes were analyzed. Part of the  
185 measurements was made with magnesium perchlorate as a dryer before the instrument inlet and part of measurements without dryer. For each measurement site, three previously evacuated 800 mL flask samples were also taken to be measured within three weeks after sampling at LSCE (Assan et al., 2017). Measurements were performed with a GC-FID (HP6890) equipped with a CP-Al<sub>2</sub>O<sub>3</sub> Na<sub>2</sub>SO<sub>4</sub> column and coupled to a preconcentrator (Entech 2007) to allow automatic injections. A standard cylinder (Messer) containing 5 non-methane hydrocarbons including ethane was used to check the stability of the instrument,  
190 while calibration was done against a reference standard from NPL (National Physics Laboratory, Teddington, UK). A previous characterization of the system had shown that the detection limit is a few ppt, the reproducibility of measurements is about 2% and the precision is better than 5% (Bonsang and Kanakidou, 2001).



### 3. Results and discussion

#### 3.1. Laboratory work

##### 195 3.1.1. Ethane calibration

During the first part of the laboratory work, the calibration slope and intercept were calculated using linear fitting of  $C_2H_6$  true (Eq. 2) versus  $C_2H_6$  observed and compared with the factors previously obtained. The calibration factors were determined after applying the interference correction (Eq. 1). Table 1 compares new calibration slopes and intercepts for the specific CRDS G2201-i device CFIDS 2072 obtained in 2018 and 2019 with previous results by Assan et al. (2017). The calibration factors have not changed significantly between 2015 and 2019.

Figure 1 shows the time series of working gas measurements with a low amount of  $C_2H_6$  during the period of December 2018 - May 2019. The  $C_2H_6$  mixing ratio does not change here significantly and is equal to  $23 \pm 12$  ppb (Figure 1). It is in contrast to Assan et al. (2017), where a time drift of the baseline was observed. This difference can be caused by fact that during previous studies, the drift was determined for corrected but not calibrated data. Here, we applied both correction and calibration before determination of time drift. Moreover, during previous studies bigger changes in determined calibration factors were observed over time. Therefore, in the following analyses, no baseline drift correction is applied.

**Table 1. Summary of the calibration factors for CRDS G2201-i device CFIDS 2072**

$C_2H_6$ calibration	Slope	Intercept [ppm]	Reference
February 2015	$0.49 \pm 0.03$	$0.00 \pm 0.01$	(Assan et al. 2017)
October 2015	$0.51 \pm 0.01$	$-0.06 \pm 0.04$	(Assan et al. 2017)
January 2018	$0.51 \pm 0.01$	$-0.03 \pm 0.01$	This study
April 2019	$0.54 \pm 0.01$	$-0.03 \pm 0.01$	This study

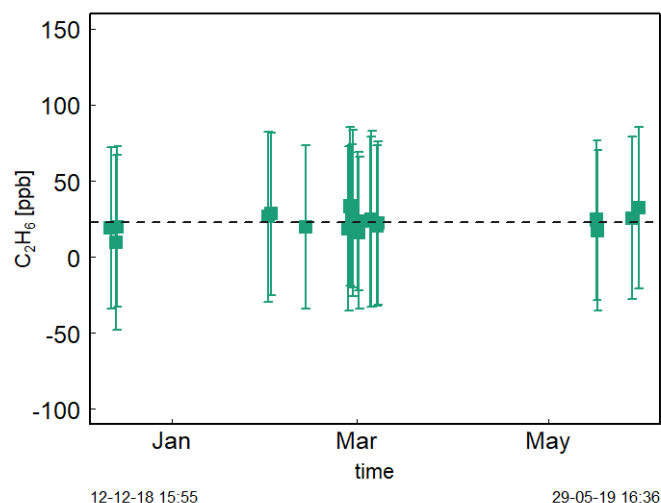


**Figure 1. Working gas 20 minutes measurements over half a year, for each measurement point: squares represent averaged value, error bars – 1 standard deviation**



### 3.1.2. CMR and Allan variance

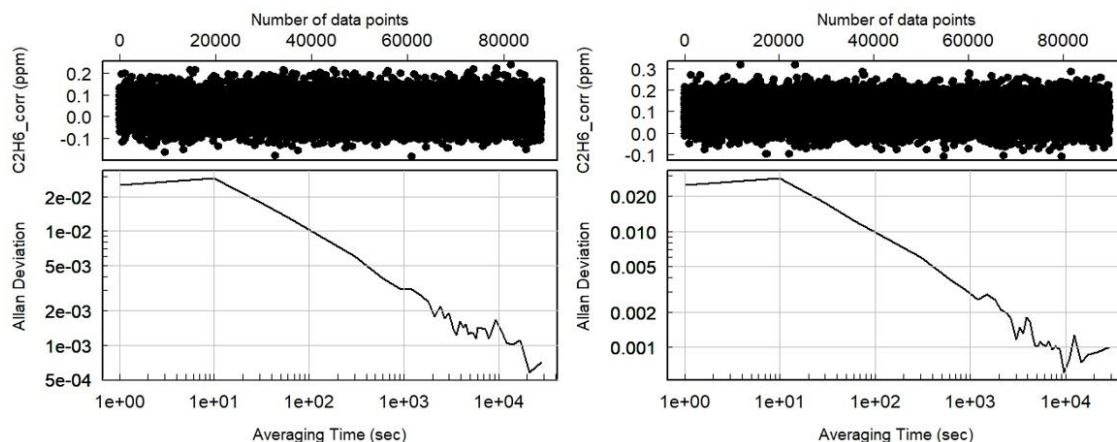
210 We determined the instrument CMR and Allan variance by measuring a working gas for 24 hours. It was also measured by  
 GC-FID coupled to a preconcentrator, and its C<sub>2</sub>H<sub>6</sub> mixing ratio equals 2.2 ppb. Using the CRDS G2201-i, the corrected and  
 calibrated value is different and steadily equals 33.2 ± 1.7 ppb over the 24 hour duration. This value suggests a bias of the  
 CRDS instrument of 31 ppb at low concentrations.

215 As the result of the 24 hour test, CMR and Allan deviation (Figure 2) are calculated for target gases with different C<sub>2</sub>H<sub>6</sub> mixing  
 ratios: low mixing ratio, 100 ppb and 1 000 ppb. In all cases, increasing the ethane mixing ratio does not affect the determined  
 CMR and Allan deviation. Looking at raw data (one data point every 3.7 s) for different mixing ratios, CMR and Allan  
 deviation are about 50 ppb and 25 ppb, respectively. Increasing averaging time improves these parameters and for 1 minute  
 average, all achieve about 13 ppb. For CRDS model G2132-i, also not dedicated to the measure of ethane (Rella et al. 2015),  
 the CMR in 1 min is about 20 ppb and Allan deviation in 1 minute is about 25 ppb. Currently, new CRDS instruments dedicated  
 220 to ethane measurements are available, for example, the CRDS 2210-i, which also measures δ<sup>13</sup>CH<sub>4</sub>. Recently (in February  
 2020), at the ICOS Atmosphere Thematic Centre (ATC) Metrology Laboratory (MLab), the CRDS G2210-i was tested and  
 for C<sub>2</sub>H<sub>6</sub> its CMR and Allan deviation are equal to 0.9 ppb and 0.8 ppb in 1 minute (ATC Mlab, personal communication).  
 The comparison between instruments are presented in Table 2

**Table 2. CMR and Allan deviation for G2201-i G2132-1 and G2210-i.**

Averaging time	Id	G2201-i Low C <sub>2</sub> H <sub>6</sub>	G2201-i ~100 ppb C <sub>2</sub> H <sub>6</sub>	G2201-i ~1000ppb C <sub>2</sub> H <sub>6</sub>	G2132-i (Rella et al., 2015)	G2210-i (ATC MLab) (personal communication)
Raw data	CMR [ppb]	51	50	50	NA	4.6
	Allan deviation [ppb]	25	25	26	NA	NA
10 second	CMR [ppb]	30	29	30	NA	NA
	Allan deviation [ppb]	29	29		NA	NA
1 minute	CMR [ppb]	13	12	12	20	0.9
	Allan deviation [ppb]	13	12	12	25	0.8



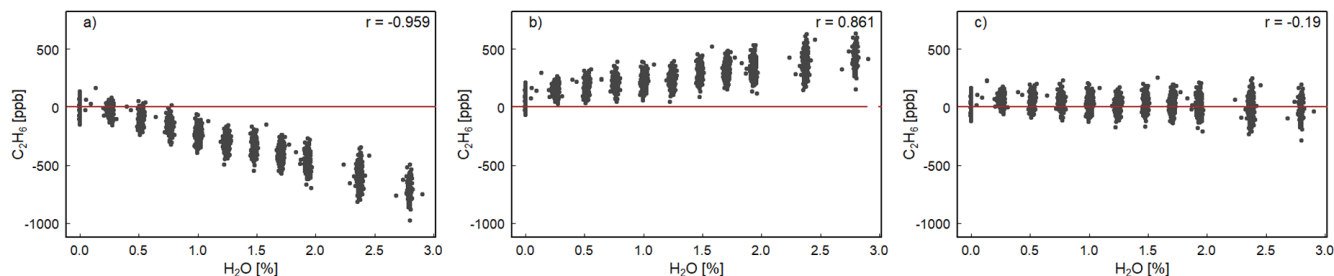


225 **Figure 2. Allan deviation for corrected and calibrated C<sub>2</sub>H<sub>6</sub>. Left: Measurement of working gas with negligible C<sub>2</sub>H<sub>6</sub> mixing ratio, right: measurement of the mixture of working gas with ~100 ppb of C<sub>2</sub>H<sub>6</sub>.**

With a 30 ppb bias and a CMR of 50 ppb, the CRDS G2201-i cannot be used to measure ethane absolute value. However, this instrument can be used to observe ethane enhancement near the source and to estimate ethane to methane ratios. From these numbers, we can deduce that the smallest enhancement that the analyzer can measure with significant precision at the highest possible data acquisition frequency is 50 ppb. This value was obtained both for gas with a low and high C<sub>2</sub>H<sub>6</sub> mixing ratio (~100 ppb and ~1 ppm). We can assume that a C<sub>2</sub>H<sub>6</sub> enhancement is significant when the maximum C<sub>2</sub>H<sub>6</sub> mixing ratio in the peak is higher than 2xSD, i.e., 100 ppb above background.

### 3.1.3. Sensitivity to water vapor

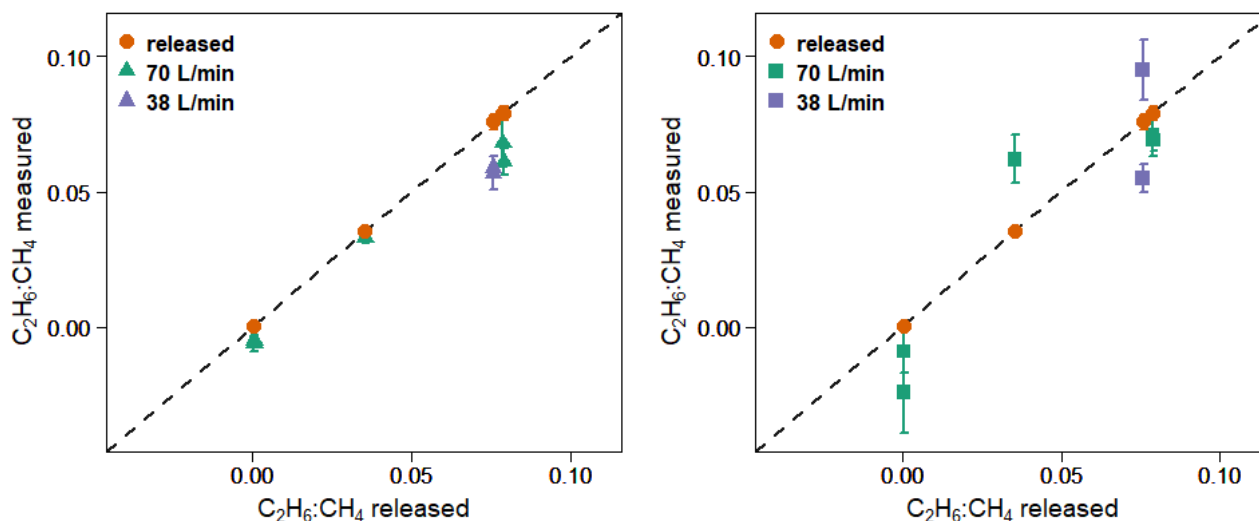
We also verified the cross-sensitivity correction proposed by Assan et al. (2017) in the presence of water vapor. Equation 1 corrects the interference of H<sub>2</sub>O, CO<sub>2</sub> and CH<sub>4</sub> in the absorption spectrum and dilution to report C<sub>2</sub>H<sub>6</sub> mixing ratio in dry air. Figure 3 shows that without interference correction (Protocol 1), the C<sub>2</sub>H<sub>6</sub> mixing ratio is underestimated and the instrument displays a negative correlation with water vapor ( $r = -0.96$ ). In Protocol 2 (high humidity interference correction), C<sub>2</sub>H<sub>6</sub> is overestimated and increases with increasing water vapor ( $r = 0.86$ ). Regarding Protocol 3 (low humidity interference correction), C<sub>2</sub>H<sub>6</sub> shows the smallest dependency on water vapor ( $r = -0.19$ ). Applying Protocol 3, the C<sub>2</sub>H<sub>6</sub> average value is  $28 \pm 61$  ppb, which is similar to the C<sub>2</sub>H<sub>6</sub> average value obtained during the previously described CMR test ( $33 \pm 51$  ppb for raw data), in dry air. Overall, according to this study, after applying Protocol 3, the water vapor has the smallest impact for observed C<sub>2</sub>H<sub>6</sub> mixing ratio and its averaged value is similar to the one obtained in the absence of water vapor. Therefore, the correction factors determined for the low humidity case (Protocol 3) should also be used in water vapor presence. Our results differ from the findings of Assan et al. (2017), where they observed changing values of the interference correction depending on the humidity. In the absence of further tests to conclude, we recommend drying air for the C<sub>2</sub>H<sub>6</sub> measurements with the CRDS G2201-i instrument. Details of the water vapor tests are presented in appendix A.



250 **Figure 3.** H<sub>2</sub>O influence on corrected C<sub>2</sub>H<sub>6</sub>. Water vapor is increased in small steps for 4 hours while measuring a target gas. The three panels show the result of applying different water correction protocols for next steps: a) no correction (Protocol 1) b) high humidity interference correction (Protocol 2) c) low humidity interference correction (Protocol 3). In all cases, for H<sub>2</sub>O = 0.00%, C<sub>2</sub>H<sub>6</sub> is corrected using low humidity interference correction. The red line represents 0 ppb.

### 3.2. Controlled release experiment

Figure 4 shows ethane to methane ratios measured in situ during the controlled release experiment (see Section 2.2). During these 7 releases, the C<sub>2</sub>H<sub>6</sub>:CH<sub>4</sub> ratio was set to ~0.032 for one release, ~0.00 for two releases and ~0.07 for four releases. For measurements with the car stopped inside the plume, most of the data from the CRDS G2201-i are found lower than known emitted C<sub>2</sub>H<sub>6</sub>:CH<sub>4</sub> ratio, (mean absolute deviation = 0.011, standard deviation = 0.004) with residuals in the range -0.018 to -0.002 for raw data (Table 3). The observed underestimation can be caused by an insufficient number of measurement points (15-20 minutes of measurement). For AirCore measurements, there is more discrepancy than for the plume standing situation, with residuals in the range -0.025 to 0.027 (mean absolute deviation = 0.017, standard deviation = 0.009). For 10 s averaged data, the range of residuals is only marginally modified, ranging from -0.019 to -0.002 and from -0.022 to 0.027 for plume standing and AirCore, respectively. Additionally, the mean absolute deviation and standard deviation are also marginally modified for both measurement situations. For example, for stationary plume standing, the absolute deviation improves marginally from 0.0111 to 0.0107. The plume standing set-up shows less noisy data and a smaller range of residuals than AirCore results. Moreover, the plume standing approach has a (small) regular bias (mean bias = -0.011), higher than in the AirCore approach (mean bias = -0.004). These results show that in the case of C<sub>2</sub>H<sub>6</sub>:CH<sub>4</sub> ratio measurements, standing inside the plume gives results closer to the reality than AirCore sampling. The example of observed CH<sub>4</sub> and C<sub>2</sub>H<sub>6</sub> mixing ratio while standing inside the peak during one of the gas releases is presented in appendix B.



270 **Figure 4.**  $C_2H_6:CH_4$  ratio observed using G2201-i as a part of a mobile setup. **Left:** measured standing inside the plumes. **Right:** measured using AirCore. Red points: known released  $C_2H_6:CH_4$  ratio. Error bars represent 1 standard deviation. The uncertainties of released values are invisible on the graph.

We also investigated the sensitivity of the  $C_2H_6:CH_4$  ratio to emission rates. During releases there were two different emission rates: 38 L/min and about 70 L/min. In the latest category, the releases while the emission rate was equal to 72 L/min and 73 L/min are grouped. The ethane to methane ratio is better estimated by the measurements for higher emission rates (bias is divided by more than 2 when increasing flow rate from ~38 to ~70 L/min). This is true both with stationary measurements and using AirCore sampler. However, only 2 different emission rates were implemented and most of the released occurred at the rate of 70 L/min, limiting the representativity of this sensitivity.

**Table 3. Residuals between measured and released  $C_2H_6:CH_4$  ratio, comparison of results made using CRDS G2201-i and LGR UMEA, AC- AirCore measurements. \* Small amount of ethane impurity in the methane**

Emitted $C_2H_6:CH_4$	emitted emission flux [L/min]	Source height [m]	LSCE CRDS G2201-i				RHUL LGR UMEA	
			n	Residuals $C_2H_6:CH_4$ 1s	Residuals $C_2H_6:CH_4$ AC 1s	Residuals $C_2H_6:CH_4$ 10s	Residuals $C_2H_6:CH_4$ AC 10s	Residuals $C_2H_6:CH_4$
$0.0355 \pm 0.0011$	70	4	382	-0.002	0.027	-0.002	0.027	-0.004
$0.0788 \pm 0.0025$	72	4	149	-0.011	-0.008	-0.009	-0.009	-0.006
$0.0790 \pm 0.0025$	73	0	220	-0.018	-0.010	-0.016	-0.010	-0.001
$0.0758 \pm 0.0028$	38	0	142	-0.017	-0.020	-0.018	-0.022	-0.007
$0.0758 \pm 0.0028$	38	4	191	-0.018	0.019	-0.019	0.020	-0.015
$0.0005 \pm 0.0006^*$	70	0	350	-0.005	-0.025	-0.005	-0.022	-0.004
$0.0005 \pm 0.0006^*$	70	4	202	-0.007	-0.010	-0.006	-0.009	-0.001
<b>Mean residuals</b>				<b>-0.011</b>	<b>0.004</b>	<b>-0.011</b>	<b>-0.004</b>	<b>-0.0051</b>

In Table 3 we also report the residuals of  $C_2H_6:CH_4$  ratio independently measured by RHUL using an LGR UMEA in another car. The residuals in  $C_2H_6:CH_4$  ratios of LGR UMEA are in the range [-0.015 to -0.001], and their mean is -0.0051 (mean absolute deviation = 0.0051). Therefore, the LGR UMEA is predictably more accurate than the CRDS G2201-i standing inside



the plumes (CRDS residuals in range -0.018 to -0.002 with mean -0.011). Despite the observed differences, results obtained by these two methods are comparable and both instruments are capable of resolving the variation of C<sub>2</sub>H<sub>6</sub>:CH<sub>4</sub> in the release experiment.

285 Additionally, three releases were measured offline using 5 liters' bag samples filled with air from the plumes. The bag samples were measured afterward in the laboratory without drying. During release one and two, emitted C<sub>2</sub>H<sub>6</sub>:CH<sub>4</sub> ratio was equal 0.00, the third release having a C<sub>2</sub>H<sub>6</sub>:CH<sub>4</sub> ratio about 0.032. In all cases, for background samples, the C<sub>2</sub>H<sub>6</sub> mixing ratio was found higher than for the bag samples collected inside the plumes. Due to that, results from the bag samples are rejected from further analysis. There are two possible reasons for the incorrect values obtained with bag samples. First, these bags could not be adapted for storing ethane. Secondly, as the samples were wet, the H<sub>2</sub>O, CO<sub>2</sub> and other species interferences on C<sub>2</sub>H<sub>6</sub> could  
 290 be higher and not linear. Thus, the applied interference correction did not improve the measured C<sub>2</sub>H<sub>6</sub> mixing ratio. In appendix C, the table of results from bag sampling is presented.

### 3.3. Field work

As a final step, the CRDS G2201-i was evaluated in real field conditions. Measurements were collected in the Paris area downwind of three gas compressor stations (referred to as A, B, C) and one landfill (D). All measurements in this section were  
 295 done stationary inside the plume.

Table 4 presents only values based on raw data (~3.7 s). We postulate that mobile applications usually aim at the highest possible acquisition frequencies. However, as the 10 s averaging increases r<sup>2</sup> fitting by about a factor two, comparison of raw data and 10 s averaged data is presented in appendix D.

**Table 4. Ratio measured at three different gas compressor stations (A, B, C) and a landfill (D); Numbers after identification letters refer to different surveys. \*: A1, B1 and B2 (wet air) and \*\* C1 (low enhancement) are rejected from further analysis (see text). ΔCH<sub>4</sub> and ΔC<sub>2</sub>H<sub>6</sub> are defined as the difference between background value (1st percentage) and the observed value inside the peak**

id	max ΔCH <sub>4</sub> [ppm]	max ΔC <sub>2</sub> H <sub>6</sub> [ppm]	C <sub>2</sub> H <sub>6</sub> :CH <sub>4</sub> ratio 1 s	r <sup>2</sup> fitting	n (data point)	Data
A2	1.737	0.269	0.060 ± 0.005	0.195	533	16.05.2019
A3	5.85	0.414	0.045 ± 0.002	0.489	495	15.07.2019
B3	1.454	0.260	0.052 ± 0.007	0.082	613	12.07.2019
B4	1.677	0.236	0.046 ± 0.008	0.086	336	12.07.2019
D1	1.516	0.266	0 ± 0.006	0	712	16.05.2019
A1*	1.486	0.309	0.070 ± 0.013	0.162	138	16.05.2019
B1*	7.314	0.878	0.090 ± 0.001	0.852	811	27.05.2019
B2*	0.513	0.323	0.085 ± 0.022	0.024	594	12.07.2019
C1**	0.495	0.284	0.091 ± 0.037	0.037	711	28.05.2019

300 Campaigns A1, B1 and B2 (Table 4) were made without using a dryer before the instrument inlet. Due to previous results that have cast doubts about the water vapor correction, the high humidity measurements have been rejected from further analysis.



Surveys B2 and C1 exhibited the highest uncertainties in the estimated ratio and the lowest correlation between the two species. These two surveys had the lowest CH<sub>4</sub> enhancements above background, about 0.5 ppm. Based on error propagation (Taylor, 1997) and using 2x CMR (100 ppb) as C<sub>2</sub>H<sub>6</sub> detection threshold, for a typical C<sub>2</sub>H<sub>6</sub>:CH<sub>4</sub> ratio of interest about 0.1, the minimal CH<sub>4</sub> enhancement above background would also be equal to 1 ppm. It suggests that a minimum CH<sub>4</sub> enhancement of 1 ppm could be required to calculate ethane to methane ratio in field conditions. As our observations are in line with the error propagation, we use 1 ppm CH<sub>4</sub> enhancement above background as a detection limit to use the CRDS G2201-i to determine ethane to methane ratio in the field conditions close to the methane source, and exclude B2 and C1 from subsequent analysis.

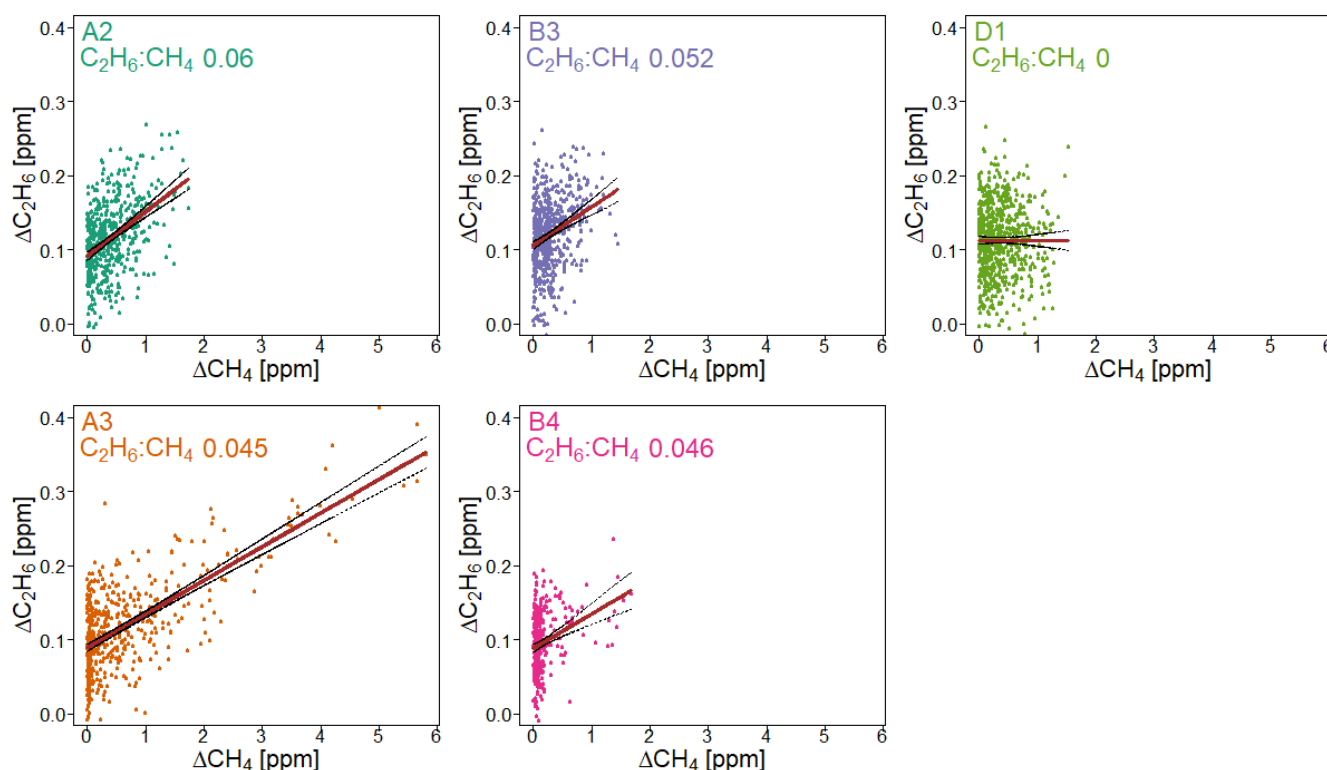


**Figure 5.** C<sub>2</sub>H<sub>6</sub>:CH<sub>4</sub> ratio for gas compressor stations (A and B) and the landfill (D), calculated for non-averaged data. Linear fitting (red line) with confidence intervals (black lines)

Figure 5 presents observations from the valid cases. We compared the observed ratios with the values provided by the owner of the gas compressor stations. The comparison is presented in Table 5. The residuals between values measured by CRDS and values provided by the owner (considered as the “true” values) are in the range -0.006 to 0.009. This range is more symmetrically distributed around the released value than for the controlled release experiment (-0.018 to 0.002, Section 3.2). The uncertainty of C<sub>2</sub>H<sub>6</sub>:CH<sub>4</sub> ratio measured using the CRDS G2201-i in the field conditions is smaller than the differences between the ratios of CH<sub>4</sub> sources (e.g., biogenic sources C<sub>2</sub>H<sub>6</sub>:CH<sub>4</sub> ~0.00, natural gas leaks and compressors stations ~0.06, processed natural gas liquids ~ 0.30). These results clearly show that C<sub>2</sub>H<sub>6</sub>:CH<sub>4</sub> ratio measured by the CRDS G2201-i can be used to portion the origin of the CH<sub>4</sub> during mobile measurements.



**Table 5. Comparison of results obtained by CRDS G2201-i with the values from the operator company.**

id	CRDS 1s C <sub>2</sub> H <sub>6</sub> :CH <sub>4</sub> ratio	Operator data C <sub>2</sub> H <sub>6</sub> :CH <sub>4</sub> ratio	Residuals C <sub>2</sub> H <sub>6</sub> :CH <sub>4</sub> ratio	Date
A2	0.060 ± 0.005	0.051	0.009	16.05.2019
A3	0.045 ± 0.002	0.049	-0.004	15.07.2019
B3	0.052 ± 0.007	0.052	0.000	12.07.2019
B4	0.046 ± 0.008	0.052	-0.006	12.07.2019
D1	0 ± 0.006	NA	NA	16.05.2019

Finally, C<sub>2</sub>H<sub>6</sub> mixing ratios measured by the CRDS G2201-i are compared with results from GC-FID. Three flask samples were taken from every surveyed site and measured afterward in the laboratory using GIC-FID. Then, the average of these three measures was calculated and for all sites their standard deviation is smaller than 1 ppb. On Figure 6, flask results are compared to results obtained by the CRDS G2201-i during the time of flask sampling. One should keep in mind that due the very short time sampling (<3s), the comparison of concentrations is only indicative. For landfill D, the C<sub>2</sub>H<sub>6</sub> mixing ratio measured by GC-FID is 4.9 ppb. For A and C gas compressor stations, the C<sub>2</sub>H<sub>6</sub> mixing ratio is 20.5 ppb and 13.7 ppb, respectively. Due to the instrument noise, for the landfill and two compressor stations (A and C), C<sub>2</sub>H<sub>6</sub> mixing ratio measured by CRDS is higher than measured by GC-FID (Figure 6) and averaged observed overestimation for these three sites is about 40 ppb. This discrepancy is similar to the one observed in laboratory conditions, where CRDS result has been higher by about 30 ppb (section 3.1). A different situation is observed in the case of the gas compressor station B where higher C<sub>2</sub>H<sub>6</sub> mixing ratio is observed. The results from flask samples are higher by about 7 ppb than from CRDS analyzer, what suggest a better agreement between instruments in the higher C<sub>2</sub>H<sub>6</sub> mixing ratio. For all sites, in the case of CRDS measurements the standard deviation is almost equal to the averaged value over the sampling time. It is caused by high instrument noise (~50 ppb CMR and 25 ppb Allan deviation for raw data) and short sampling time (less than one minute).

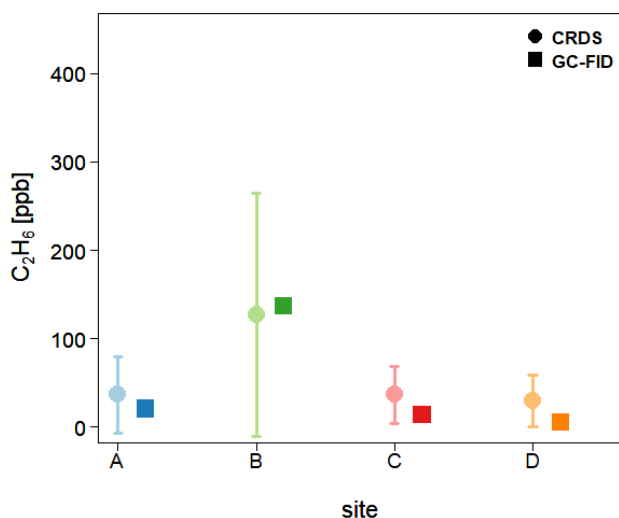




**Figure 6. Comparison of the C<sub>2</sub>H<sub>6</sub> mixing ratio measured in-situ by CRDS G2201-i and in the laboratory by GC-FID from flasks measurements. CRDS G2201-i measurements during the time of flask sampling. Uncertainties (1 SD) are indicated both for CRDS and GC-FID.**

#### 335 4. Discussion: Overall comparison with other instruments and methods

Based on the series of tests conducted in our study, using the CRDS G2201-i in a mobile set-up to measure C<sub>2</sub>H<sub>6</sub>:CH<sub>4</sub> ratio in methane plumes appears possible and can provide useful scientific results under specific conditions. In laboratory conditions, during measurements of gas containing C<sub>2</sub>H<sub>6</sub>, the CRDS G2201-i has a better CMR (12 ppb in 1 min) and a smaller noise calculated from Allan deviation (~10 ppb in 1 min) than the CRDS G2132-i, which are equal 20 ppb and 25 ppb, respectively, in 1 min timeframe (Rella et al. 2015), where both instruments are not dedicated for C<sub>2</sub>H<sub>6</sub> measurements. However, both instruments have lower performance than the CRDS G2210-i, dedicated to C<sub>2</sub>H<sub>6</sub> measurement. For the latter instrument, both CMR and Allan deviation are smaller than 1 ppb (ATC Mlab test, personal communication). Additionally, based on a literature comparison, for both CRDS instruments, CMR and noise are higher than those obtained for the instrument based on the TLDAS method, dedicated for mobile measurements of C<sub>2</sub>H<sub>6</sub> (as described by Yacovitch et al. 2014). For that instrument, the CMR is as low as 19 ppt in stationary conditions, and 210 ppt in motion.

Based on Assan et al. (2017), the correction of the sensitivity to other species is necessary (Eq. (1)) to account for the different instrument responses to water level lower or higher than 0.16% (low and high humidity). In this study, during laboratory work, the water vapor sensitivity was evaluated and results showed that applying interference correction factors determined for low humidity gave better results, including for more humidified air measurements. It is in opposition to results obtained by Assan et al. (2017). Therefore, we consider that water presence should be avoided and we recommend drying air before C<sub>2</sub>H<sub>6</sub> measurement using CRDS G2201-i.

Previously, the CRDS G2201-i device CFIDS 2072 has only been used in stationary field work over two weeks (Assan et al. 2017) to make continuous measurements of CH<sub>4</sub>, δ<sup>13</sup>CH<sub>4</sub> and C<sub>2</sub>H<sub>6</sub> from gas facilities. The CRDS G2201-i and GC-FID measured air simultaneously from the shared inlet and were located 200 – 400 m from the gas facilities (pipelines and compressors). The GC-FID used in Assan et al. (2017) was a field instrument described in Gros et al. (2011) and Panopoulou et al. (2018) which has an overall uncertainty estimated to be better than 15%. For GC-FID 10 minutes of ambient air collection was measured during 20 minutes. Thus, for that instrument, the sampling time is 10 minutes sampling average over 30 minutes. To have identical timestamps as GC-FID, corrected and calibrated CRDS data were averaged for 10 min every 30 min. Flask samples were taken as well during that field work. That study was the first attempt to propose a protocol to use CRDS G2201-i to measure C<sub>2</sub>H<sub>6</sub>:CH<sub>4</sub> ratio, both from flask sampling and from continuous measurements, and found a good agreement between CRDS and GC-FID measurements (Assan et al. 2017). In our study, we went one step further and considered the constraints associated with a mobile setup within a car. As the instrument noise increases during the motion of the car, we decided to stop the car for about 35 minutes inside the plume to acquire the observations. As it is not possible to stop the car in every place where measurements are made, it is a limitation for this application of the instrument, compared to other



365 instruments able to measure  $C_2H_6$  while moving across the plume, like the LGR UMEA (Lowry et al. 2020) or the instrument based on TILDAS method (Smith et al., 2015; Yacovitch et al., 2014, 2020).

During our trace release experiment,  $C_2H_6:CH_4$  ratio was calculated from measurements made when the car was standing inside the plume. With this approach, measured ratios were underestimated. However, using the LGR UMEA instrument, dedicated to mobile  $C_2H_6:CH_4$  ratio measurements, some discrepancy between the measured and released value was also  
370 observed, albeit smaller. Indeed, in the case of the LGR UMEA measurements, the residuals between measurements and released value were in the range -0.015 to -0.001, where using the CRDS G2201-i the residuals are in the range -0.018 to -0.002. It is also worth noting that the more precise instrument, presented by Yacovitch et al. (2014), also inferred a systematical underestimation of the  $C_2H_6$  mixing ratio by ~6% of the measured value. In their study, this systematic error was added as a reported statistical error (Yacovitch et al. 2014).

375 In our study, during the trace release experiment, we also compared results obtained by stationary standing inside the plume and by sampling air with an AirCore system. The absolute deviation is equal to 0.011 and 0.017 for stationary mode and AirCore mode, respectively. The residuals between released and measured values are from -0.018 to -0.002 for stationary mode and from -0.025 to 0.027 for AirCore mode. Thus, the agreement with released  $C_2H_6:CH_4$  ratio is better for measurements made by standing inside the plumes than with AirCore sampler. However, during previous studies where CRDS instruments  
380 were used (Rella et al. 2015; Lopez et al. 2017),  $C_2H_6:CH_4$  ratio was also measured using AirCore sampler. In the study made by Lopez et al. (2017) for pipelines measurements, gas flasks were also collected and measured at INSTAAR (Boulder, CO, USA) using gas chromatography. Overall, AirCore sampler results were in good agreement with the results for flasks measurements. During these measurements, the CRDS was flushed continuously with a flow rate of 1000 mL/min and a mass flow controller was part of the setup. During AirCore analysis, the airflow rate was equal to 40 mL/min. This change allowed  
385 to increase the number of measurements point by 25, when the replay mode was used. In our study, in the monitoring mode, we flushed the CRDS instrument with a flow rate of 160 mL/min and in the replay mode, we increased the number of points only by 3. These differences could contribute to explaining the discrepancies between measured and released  $C_2H_6:CH_4$  ratio. Further decreasing the flow rate will increase the number of sampling points and could improve the agreement between AirCore-based estimations and actual ratios. This should be tested to conclude the optimal use of AirCore setup to improve  
390 the characterization of methane sources.

Finally, the  $C_2H_6:CH_4$  ratios obtained by standing inside the plumes are accurate and allow to separate the different releases at the resolution of the conducted experiment. They are also comparable with results obtained using LGR UMEA. This agreement between measurements and reality has also been confirmed during real field conditions mobile measurements. During these measurements, residuals for dry air sampling were between -0.006 and 0.009. Additionally, during field work, flasks samples  
395 have been taken and measured by GC-FID in the laboratory. During the time of flask sampling at the two gas compressors stations, the  $C_2H_6$  mixing ratios were below the value of the instrument CMR (~50 ppb). For the third gas compressor station, the  $C_2H_6$  mixing ratio was above the detection threshold and  $C_2H_6$  mixing ratio measured by GC-FID was higher than measured by CRDS. Nevertheless, due to the short sampling time of the flasks, these first comparisons are only indicative and more





comparison campaigns should help to understand the discrepancies between these instruments. In all cases, the standard  
400 deviation of  $C_2H_6$  measured by CRDS was close to the averaged value. It shows the CRDS G2201-i should not be used for the  
measurements of the absolute value of the  $C_2H_6$  mixing ratio.

Overall, using  $C_2H_6:CH_4$  ratio measured by the CRDS G2201-i, it is possible to separate methane sources between a biogenic  
origin ( $C_2H_6:CH_4 \sim 0.00$ ), natural gas leaks and compressors ( $C_2H_6:CH_4 \sim 0.06$ , can vary between 0.02-0.17) and processed  
405 natural gas liquids ( $C_2H_6:CH_4 \sim 0.3$ ).  $C_2H_6:CH_4$  ratio of natural gas can vary on origin and processing. Thus, determining the  
exact source of methane inside the industrial site, with a lot of potential methane emitters, can be more challenging to achieve.  
However, looking at the results of our study, if the differences between  $C_2H_6:CH_4$  ratios are higher than 0.01, it is still possible  
to determine the source of the observed  $CH_4$  plume using  $C_2H_6:CH_4$  ratio measured by the CRDS G2201-i.

## 5. Conclusions

The instrument CRDS G2201-i measures  $^{12}CO_2$ ,  $^{13}CO_2$ ,  $^{12}CH_4$ ,  $^{13}CH_4$ ,  $H_2O$  and  $C_2H_6$ , the latter being initially present to correct  
410  $^{13}CH_4$  measurements. This study investigates the possibility to make ethane measurements, made by a CRDS G2201-i  
instrument, useful for methane source apportionment. The interest is to be able to better constrain methane sources at the  
laboratory and in the field with only one instrument. Before any analysis,  $C_2H_6$  raw data must be corrected and calibrated. The  
linearity test showed good stability over time, with only a small change of calibration factors over 4 years. Contrary to the  
previous studies (Rella et al. 2015; Assan et al. 2017), we do not observe any time drift of the  $C_2H_6$  baseline. Nevertheless,  
415 regular calibrations and target measurements are advised.

The controlled release experiment revealed a small systematical underestimation of measured ratios inside the plumes  
compared to released ones. The larger discrepancy from released  $C_2H_6:CH_4$  occurs in the case of AirCore samplings. Due to  
that, we recommend standing inside the plumes instead of taking AirCore samples to measure  $C_2H_6:CH_4$  ratios. However,  
decreasing the flushing flow rate of the CRDS can improve the performance of the instrument during AirCore sampling and  
420 should be further investigated in the next campaigns.

In this study, we find some limitations of using CRDS G2201-i to measure  $C_2H_6:CH_4$ . First of all, we found that we need at  
least a peak maximum of 100 ppb in ethane to get useful results to help portioning methane sources. Additionally, the required  
maximum  $CH_4$  enhancement above background should be higher than 1 ppm. This threshold is determined using error  
propagation for a typical  $C_2H_6:CH_4$  ratio equal to 0.1. In the field conditions, this threshold was successfully used for  $C_2H_6:CH_4$   
425 ratio close to 0.05. For weak sources with enhancements below 1 ppm, this limitation prevents providing  $C_2H_6:CH_4$  ratio  
measurements using our approach. Secondly, we have observed significant changes in observed  $C_2H_6$  mixing ratios in the  
presence of water vapor and we strongly recommend drying air before making measurements.

Third, due to an increase of the instrument noise during the motion of the car, it is not possible to measure  $C_2H_6:CH_4$  ratio  
when moving across plumes as currently made to estimate methane emissions (e.g., Ars et al. 2017). Other dedicated



430 instruments have to be used in this case for ethane (Yacovitch et al. 2014; Lowry et al. 2020). To fix this problem,  $C_2H_6:CH_4$   
ratio can be measured by standing inside the plumes or by AirCore sampling after solving the flushing issue.  
Despite these limitations, this study shows the possibility of using the CRDS G2201-i to measure  $C_2H_6:CH_4$  ratio in the field  
conditions in strong methane enhancements, using mobile platforms. Even though the instrument is not dedicated for  $C_2H_6:CH_4$   
ratio measurements, after applying correction and calibration factors, when the air is dried and methane maximum in a peak is  
435 1 ppm above background, the CRDS G2201-i gives results comparable with released values in controlled experiments.  
Therefore, under these conditions, the CRDS G2201-i instrument can contribute to better constrain methane sources deploying  
only one instrument.

## Appendix A

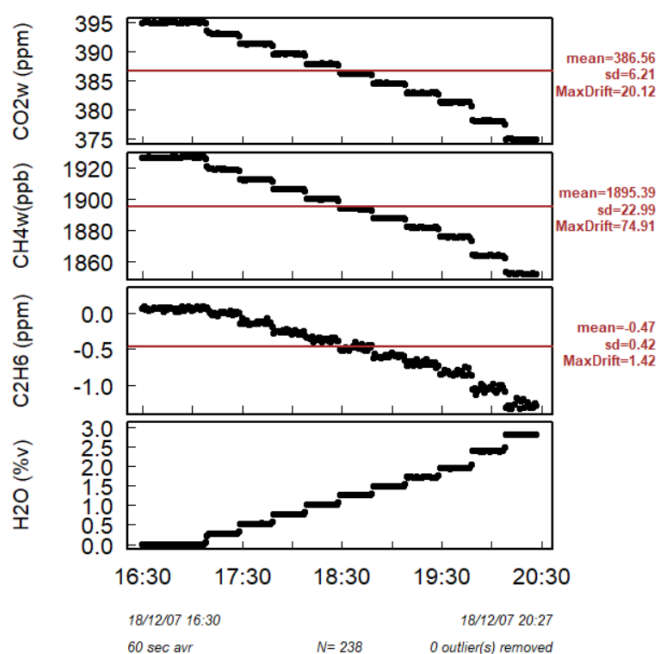


**Figure A1. H<sub>2</sub>O influence on CO<sub>2</sub>, CH<sub>4</sub> and C<sub>2</sub>H<sub>6</sub>.**

440 The results, presented in Figure 3 in the paper, were obtained using wet CH<sub>4</sub> and CO<sub>2</sub> values. In the next step, the analysis of  
the water vapor sensitivity test was repeated using dry CH<sub>4</sub> and CO<sub>2</sub> values. These dry values are corrected by default already  
in the instrument. For all three cases, using dry or wet CH<sub>4</sub> and CO<sub>2</sub> values did not change the C<sub>2</sub>H<sub>6</sub> values, which suggests a  
bigger influence of H<sub>2</sub>O than CH<sub>4</sub> and CO<sub>2</sub> on C<sub>2</sub>H<sub>6</sub>. When the interference correction for low humidity was applied for all  
steps, the average C<sub>2</sub>H<sub>6</sub> mixing ratio is equal  $28 \pm 62$  ppb and  $28 \pm 61$  ppb for wet and dry CH<sub>4</sub> and CO<sub>2</sub>, respectively. Figure  
445 A2 presents a comparison of wet and dry CO<sub>2</sub> and CH<sub>4</sub> values.

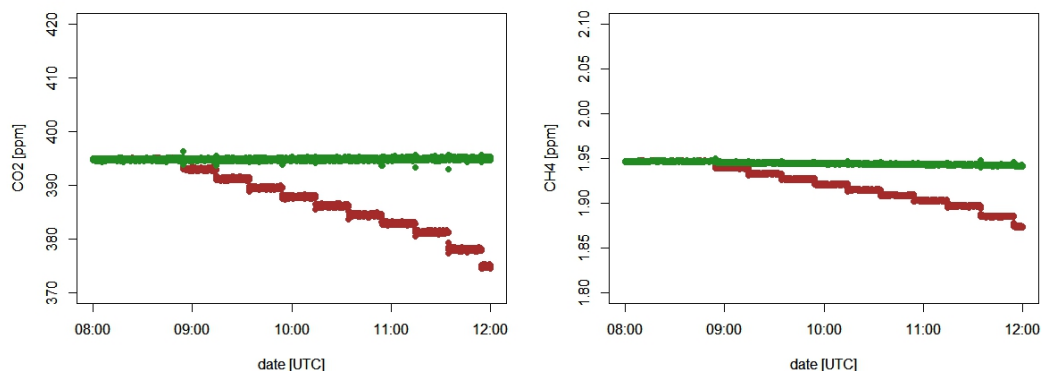


Figure A2. Dry (manufactured correction) and wet values of CO<sub>2</sub> and CH<sub>4</sub>. Green – dry values, red – wet values. Left: CO<sub>2</sub> mixing ratio, right CH<sub>4</sub> mixing ratio.

## Appendix B

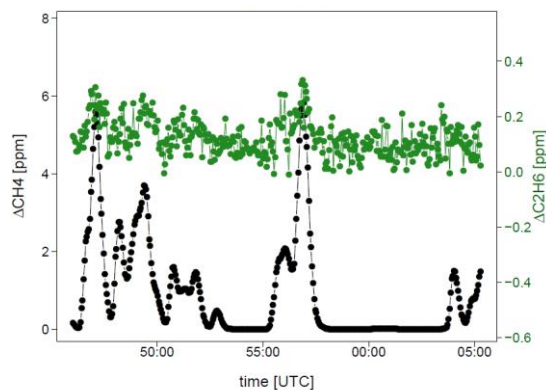
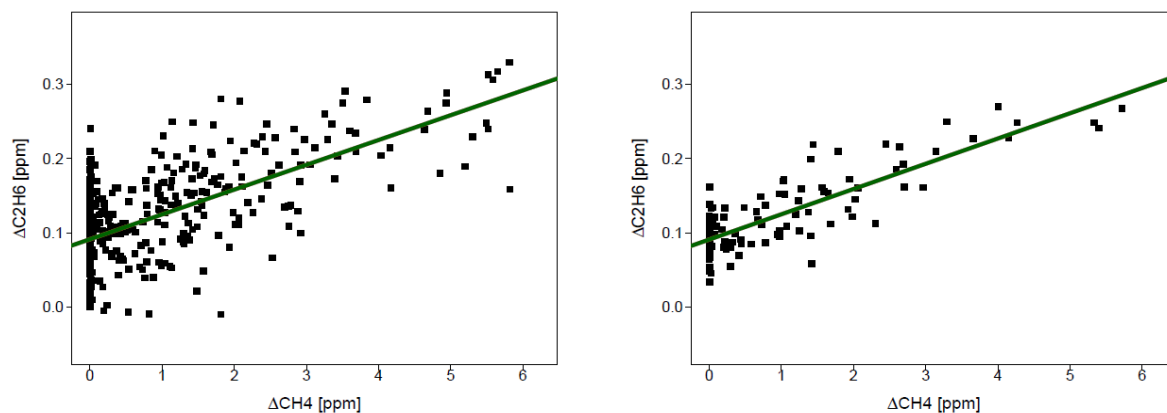


Figure B1. CH<sub>4</sub> and C<sub>2</sub>H<sub>6</sub> mixing ratio observed during standing inside the plume



450 Figure B2. C<sub>2</sub>H<sub>6</sub> mixing ratio vs. CH<sub>4</sub> mixing ratio observed while standing inside the plume. Left: non-averaged data. Right: 10 s averaged data. Green line: linear fitting



## Appendix C

**Table C1 C<sub>2</sub>H<sub>6</sub>:CH<sub>4</sub> ratio with interference correction for high humidity. \* background samples**

name.id	CO <sub>2</sub> [ppm]	CH <sub>4</sub> [ppm]	δ <sup>13</sup> CH <sub>4</sub> [‰]	H <sub>2</sub> O [%]	C <sub>2</sub> H <sub>6</sub> [ppm]	C <sub>2</sub> H <sub>6</sub> :CH <sub>4</sub> ratio
1.1b	402	2.23	-47	1.25	0.27 ± 0.06	0.12 ± 0.03
1.2b	397	2.01	-47	1.22	0.27 ± 0.06	0.13 ± 0.03
1.3b	399	3.34	-45	1.22	0.39 ± 0.06	0.12 ± 0.02
1.4b*	395	1.96	-48	1.23	0.44 ± 0.06	0.22 ± 0.03
1.5b	399	2.31	-46	1.29	0.43 ± 0.06	0.19 ± 0.03
1.6b	399	5.25	-43	1.29	0.45 ± 0.07	0.09 ± 0.01
1.7b	402	5.19	-44	1.29	0.62 ± 0.09	0.12 ± 0.02
1.8b*	396	1.98	-48	1.25	0.55 ± 0.08	0.28 ± 0.04
2.1b	420	3.25	-45	1.27	0.55 ± 0.07	0.17 ± 0.02
2.2b*	397	1.97	-49	1.17	0.72 ± 0.15	0.36 ± 0.08

## Appendix D

Comparison of raw data and 10 s averaged data from measurements in the Ile-de-France region

**Table D1. Field work analysis A, B and C- gas compressor, BB – landfill; \*: A1, B1 and B2 rejected from further analysis (wet air) and \*\*: C1 rejected from further analysis (low enhancement), raw and 10 s averaged data**

id	max ΔCH <sub>4</sub>	max ΔC <sub>2</sub> H <sub>6</sub>	1 s	r <sup>2</sup>	10 s	r <sub>2</sub>	n	data
A1*	1.486	0.309	0.070 ± 0.013	0.162	0.066 ± 0.018	0.235	138	16.05.2019
A2	1.737	0.269	0.060 ± 0.005	0.195	0.059 ± 0.007	0.303	533	16.05.2019
A3	5.85	0.414	0.045 ± 0.002	0.489	0.044 ± 0.003	0.645	495	15.07.2019
B1*	7.314	0.878	0.090 ± 0.001	0.852	0.091 ± 0.002	0.927	811	27.05.2019
B2*	0.513	0.323	0.085 ± 0.022	0.024	0.083 ± 0.029	0.044	594	12.07.2019
B3	1.454	0.26	0.052 ± 0.007	0.082	0.05 ± 0.009	0.15	613	12.07.2019
B4	1.677	0.236	0.046 ± 0.008	0.086	0.05 ± 0.011	0.174	336	12.07.2019
C1**	0.495	0.284	0.091 ± 0.037	0.037	0.09 ± 0.021	0.082	711	28.05.2019
D1	1.516	0.266	0 ± 0.006	0	0 ± 0.007	0	712	16.05.2019

## 455 Data availability

Data from the field work and most of the laboratory tests are available on the Carbon Portal and waiting to obtain a DOI number. Data from time drift test are available on demand.



### Author contribution

Conceptualization, S.D., J.D.P.; Methodology, S.D., J.D.P. C.Y.K., D.L., J.F., J.H., N.Y, V.G.; Software, S.D., C.Y.K., D.L.;  
460 Formal Analysis, S.D., D.L., N.Y.; Investigation, S.D., J.D.P. C.Y.K., D.L.; Resources, J.D.P. C.Y.K., P.B., J.H.; Data Curation  
S.D., D.L.; Writing – Original, S.D.; Draft Writing – Review & Editing, S.D., J.D.P. C.Y.K., D.L., J.F., J.H., N.Y. V.G., P.B.;  
Visualization, S.D., D.L.; Supervision, J.D.P. C.Y.K., P.B.

### Competing interests

The authors declare that they have no conflict of interest.

### 465 Acknowledgments

We acknowledge our laboratory colleagues C. Philippon and L. Lienhardt, for sharing results of tests made in ATC Mlab. We  
thank also gratefully D. Baisnee for the measurements of flask samples on the GC-FID. We gratefully acknowledge GRTgaz  
company for sharing data with us and helping to improve the manuscript, especially: P. Guillo-Lohan, P. Alas, F. Bainier and  
JL. Fabre.

### 470 References

- Allan, D. W.: Statistics of atomic frequency standards, *Proc. IEEE*, 54(2), 221–230, doi:10.1109/PROC.1966.4634, 1966.
- Assan, S., Baudic, A., Guemri, A., Ciaï, P., Gros, V. and Vogel, F. R.: Characterization of interferences to in situ observations  
of delta13CH4 and C2H6 when using a cavity ring-down spectrometer at industrial sites, *Atmospheric Measurement  
Techniques*, 10(6), 2077–2091, doi:10.5194/amt-10-2077-2017, 2017.
- 475 Aydin, M., Verhulst, K. R., Saltzman, E. S., Battle, M. O., Montzka, S. A., Blake, D. R., Tang, Q. and Prather, M. J.: Recent  
decreases in fossil-fuel emissions of ethane and methane derived from firn air, *Nature*, 476(7359), 198–201,  
doi:10.1038/nature10352, 2011.
- Bonsang, B. and Kanakidou, M.: Non-methane hydrocarbon variability during the FIELDVOC'94 campaign in Portugal,  
*Chemosphere - Global Change Science*, 3(3), 259–273, doi:10.1016/S1465-9972(01)00009-5, 2001.
- 480 Bourtsoukidis, E., Ernle, L., Crowley, J. N., Lelieveld, J., Paris, J.-D., Pozzer, A., Walter, D. and Williams, J.: Non Methane  
Hydrocarbon sources and sinks around the Arabian Peninsula, *Atmospheric Chemistry and Physics Discussions*, 1–45,  
doi:https://doi.org/10.5194/acp-2019-92, 2019.
- Defratyka, S., Paris, J. D., Yver-Kwok, C., Fernandez, J. M., Korben, P. and Bousquet, P.: Mapping urban methane sources in  
Paris, France, Manuscript submitted for publication, 2020.
- 485 Dlugokencky, E.: NOAA/ESRL, 2020.



- Gardiner, T., Helmore, J., Innocenti, F. and Robinson, R.: Field Validation of Remote Sensing Methane Emission Measurements, *Remote Sensing*, 9(9), 956, doi:10.3390/rs9090956, 2017.
- Gros, V., Gaimoz, C., Herrmann, F., Custer, T., Williams, J., Bonsang, B., Sauvage, S., Locoge, N., d'Argouges, O., Sarda-Estève, R. and Sciare, J.: Volatile organic compounds sources in Paris in spring 2007. Part I: qualitative analysis, *Environ. Chem.*, 8(1), 74, doi:10.1071/EN10068, 2011.
- 490 Hausmann, P., Sussmann, R. and Smale, D.: Contribution of oil and natural gas production to renewed increase in atmospheric methane (2007–2014): top–down estimate from ethane and methane column observations, *Atmos. Chem. Phys.*, 16(5), 3227–3244, doi:10.5194/acp-16-3227-2016, 2016.
- Helmig, D., Rossabi, S., Hueber, J., Tans, P., Montzka, S. A., Masarie, K., Thoning, K., Plass-Duelmer, C., Claude, A., Carpenter, L. J., Lewis, A. C., Punjabi, S., Reimann, S., Vollmer, M. K., Steinbrecher, R., Hannigan, J. W., Emmons, L. K., Mahieu, E., Franco, B., Smale, D. and Pozzer, A.: Reversal of global atmospheric ethane and propane trends largely due to US oil and natural gas production, *Nature Geosci*, 9(7), 490–495, doi:10.1038/ngeo2721, 2016.
- 495 Hoheisel, A.: Characterisation of delta13CH4 source signatures from methane sources in Germany using mobile measurements, University of Heidelberg, Institute of Environmental Physics, 1 October., 2018.
- 500 Hoheisel, A., Yeman, C., Dinger, F., Eckhardt, H. and Schmidt, M.: An improved method for mobile characterisation of  $\delta^{13}\text{CH}_4$  source signatures and its application in Germany, *Atmospheric Measurement Techniques*, 12(2), 1123–1139, doi:<https://doi.org/10.5194/amt-12-1123-2019>, 2019.
- IPCC: Climate Change 2013: The Physical Science Basis. Contribution of Working Group I to the Fifth Assessment Report of the Intergovernmental Panel on Climate Change, Cambridge University Press, Cambridge, United Kingdom and New York, NY, USA., 2018.
- 505 Kort, E. A., Smith, M. L., Murray, L. T., Gvakharia, A., Brandt, A. R., Peischl, J., Ryerson, T. B., Sweeney, C. and Travis, K.: Fugitive emissions from the Bakken shale illustrate role of shale production in global ethane shift: Ethane Emissions From the Bakken Shale, *Geophys. Res. Lett.*, 43(9), 4617–4623, doi:10.1002/2016GL068703, 2016.
- Lopez, M., Sherwood, O. A., Dlugokencky, E. J., Kessler, R., Giroux, L. and Worthy, D. E. J.: Isotopic signatures of anthropogenic CH<sub>4</sub> sources in Alberta, Canada, *Atmospheric Environment*, 164, 280–288, doi:10.1016/j.atmosenv.2017.06.021, 2017.
- 510 Lowry, D., Fisher, R. E., France, J. L., Coleman, M., Lanoisellé, M., Zazzeri, G., Nisbet, E. G., Shaw, J. T., Allen, G., Pitt, J. and Ward, R. S.: Environmental baseline monitoring for shale gas development in the UK: Identification and geochemical characterisation of local source emissions of methane to atmosphere, *Science of The Total Environment*, 708, 134600, doi:10.1016/j.scitotenv.2019.134600, 2020.
- 515 McKain, K., Down, A., Raciti, S. M., Budney, J., Hutyrá, L. R., Floerchinger, C., Herndon, S. C., Nehrkorn, T., Zahniser, M. S., Jackson, R. B., Phillips, N. and Wofsy, S. C.: Methane emissions from natural gas infrastructure and use in the urban region of Boston, Massachusetts, *Proceedings of the National Academy of Sciences*, 112(7), 1941–1946, doi:10.1073/pnas.1416261112, 2015.
- 520 Panopoulou, A., Liakakou, E., Gros, V., Sauvage, S., Locoge, N., Bonsang, B., Psiloglou, B. E., Gerasopoulos, E. and Mihalopoulos, N.: Non-methane hydrocarbon variability in Athens during wintertime: the role of traffic and heating, *Atmos. Chem. Phys.*, 18(21), 16139–16154, doi:10.5194/acp-18-16139-2018, 2018.



- 525 Rella, C. W., Hoffnagle, J., He, Y. and Tajima, S.: Local- and regional-scale measurements of CH<sub>4</sub>, δ<sup>13</sup>CH<sub>4</sub>, and C<sub>2</sub>H<sub>6</sub> in the Uintah Basin using a mobile stable isotope analyzer, *Atmospheric Measurement Techniques*, 8(10), 4539–4559, doi:10.5194/amt-8-4539-2015, 2015.
- 530 Saunois, M., Bousquet, P., Poulter, B., Peregon, A., Ciais, P., Canadell, J. G., Dlugokencky, E. J., Etiope, G., Bastviken, D., Houweling, S., Janssens-Maenhout, G., Tubiello, F. N., Castaldi, S., Jackson, R. B., Alexe, M., Arora, V. K., Beerling, D. J., Bergamaschi, P., Blake, D. R., Brailsford, G., Brovkin, V., Bruhwiler, L., Crevoisier, C., Crill, P., Covey, K., Curry, C., Frankenberg, C., Gedney, N., Höglund-Isaksson, L., Ishizawa, M., Ito, A., Joos, F., Kim, H.-S., Kleinen, T., Krummel, P., Lamarque, J.-F., Langenfelds, R., Locatelli, R., Machida, T., Maksyutov, S., McDonald, K. C., Marshall, J., Melton, J. R., Morino, I., Naik, V., O’Doherty, S., Parmentier, F.-J. W., Patra, P. K., Peng, C., Peng, S., Peters, G. P., Pison, I., Prigent, C., Prinn, R., Ramonet, M., Riley, W. J., Saito, M., Santini, M., Schroeder, R., Simpson, I. J., Spahni, R., Steele, P., Takizawa, A., Thornton, B. F., Tian, H., Tohjima, Y., Viovy, N., Voulgarakis, A., van Weele, M., van der Werf, G. R., Weiss, R., Wiedinmyer, C., Wilton, D. J., Wiltshire, A., Worthy, D., Wunch, D., Xu, X., Yoshida, Y., Zhang, B., Zhang, Z. and Zhu, Q.: The global methane budget 2000–2012, *Earth System Science Data*, 8(2), 697–751, doi:10.5194/essd-8-697-2016, 2016.
- 540 Saunois, M., Stavert, A. R., Poulter, B., Bousquet, P., Canadell, J. G., Jackson, R. B., Raymond, P. A., Dlugokencky, E. J., Houweling, S., Patra, P. K., Ciais, P., Arora, V. K., Bastviken, D., Bergamaschi, P., Blake, D. R., Brailsford, G., Bruhwiler, L., Carlson, K. M., Carrol, M., Castaldi, S., Chandra, N., Crevoisier, C., Crill, P. M., Covey, K., Curry, C. L., Etiope, G., Frankenberg, C., Gedney, N., Hegglin, M. I., Höglund-Isaksson, L., Hugelius, G., Ishizawa, M., Ito, A., Janssens-Maenhout, G., Jensen, K. M., Joos, F., Kleinen, T., Krummel, P. B., Langenfelds, R. L., Laruelle, G. G., Liu, L., Machida, T., Maksyutov, S., McDonald, K. C., McNorton, J., Miller, P. A., Melton, J. R., Morino, I., Müller, J., Murgia-Flores, F., Naik, V., Niwa, Y., Noce, S., O’Doherty, S., Parker, R. J., Peng, C., Peng, S., Peters, G. P., Prigent, C., Prinn, R., Ramonet, M., Regnier, P., Riley, W. J., Rosentreter, J. A., Segers, A., Simpson, I. J., Shi, H., Smith, S. J., Steele, L. P., Thornton, B. F., Tian, H., Tohjima, Y., Tubiello, F. N., Tsuruta, A., Viovy, N., Voulgarakis, A., Weber, T. S., van Weele, M., van der Werf, G. R., Weiss, R. F., 545 Worthy, D., Wunch, D., Yin, Y., Yoshida, Y., Zhang, W., Zhang, Z., Zhao, Y., Zheng, B., Zhu, Q., Zhu, Q. and Zhuang, Q.: The Global Methane Budget 2000–2017, preprint, *Atmosphere – Atmospheric Chemistry and Physics*, 2020.
- Schwietzke, S., Griffin, W. M., Matthews, H. S. and Bruhwiler, L. M. P.: Natural Gas Fugitive Emissions Rates Constrained by Global Atmospheric Methane and Ethane, *Environ. Sci. Technol.*, 48(14), 7714–7722, doi:10.1021/es501204c, 2014.
- 550 Sherwood, O. A., Schwietzke, S., Arling, V. A. and Etiope, G.: Global Inventory of Gas Geochemistry Data from Fossil Fuel, Microbial and Burning Sources, version 2017, *Earth Syst. Sci. Data*, 9(2), 639–656, doi:10.5194/essd-9-639-2017, 2017.
- Simpson, I. J., Sulbaek Andersen, M. P., Meinardi, S., Bruhwiler, L., Blake, N. J., Helmig, D., Rowland, F. S. and Blake, D. R.: Long-term decline of global atmospheric ethane concentrations and implications for methane, *Nature*, 488(7412), 490–494, doi:10.1038/nature11342, 2012.
- 555 Smith, M. L., Kort, E. A., Karion, A., Sweeney, C., Herndon, S. C. and Yacovitch, T. I.: Airborne Ethane Observations in the Barnett Shale: Quantification of Ethane Flux and Attribution of Methane Emissions, *Environ. Sci. Technol.*, 49(13), 8158–8166, doi:10.1021/acs.est.5b00219, 2015.
- Taylor, J. R.: An introduction to error analysis. The study of uncertainties in physical measurements, second., University Science Books., 1997.
- 560 Turner, A. J., Frankenberg, C. and Kort, E. A.: Interpreting contemporary trends in atmospheric methane, *Proc Natl Acad Sci USA*, 116(8), 2805–2813, doi:10.1073/pnas.1814297116, 2019.
- Yacovitch, T. I., Herndon, S. C., Roscioli, J. R., Floerchinger, C., McGovern, R. M., Agnese, M., Pétron, G., Kofler, J., Sweeney, C., Karion, A., Conley, S. A., Kort, E. A., Nöhle, L., Fischer, M., Hildebrandt, L., Koeth, J., McManus, J. B., Nelson,



- D. D., Zahniser, M. S. and Kolb, C. E.: Demonstration of an Ethane Spectrometer for Methane Source Identification, *Environ. Sci. Technol.*, 48(14), 8028–8034, doi:10.1021/es501475q, 2014.
- 565 Yacovitch, T. I., Daube, C. and Herndon, S. C.: Methane Emissions from Offshore Oil and Gas Platforms in the Gulf of Mexico, *Environ. Sci. Technol.*, 54(6), 3530–3538, doi:10.1021/acs.est.9b07148, 2020.
- Yang, K., Ting, C., Wang, J., Wingenter, O. and Chan, C.: Diurnal and seasonal cycles of ozone precursors observed from continuous measurement at an urban site in Taiwan, *Atmospheric Environment*, 39(18), 3221–3230, doi:10.1016/j.atmosenv.2005.02.003, 2005.
- 570 Yver Kwok, C., Laurent, O., Guemri, A., Philippon, C., Wastine, B., Rella, C. W., Vuillemin, C., Truong, F., Delmotte, M., Kazan, V., Darding, M., Lebègue, B., Kaiser, C., Xueref-Rémy, I. and Ramonet, M.: Comprehensive laboratory and field testing of cavity ring-down spectroscopy analyzers measuring H<sub>2</sub>O, CO<sub>2</sub>, CH<sub>4</sub> and CO, *Atmos. Meas. Tech.*, 8(9), 3867–3892, doi:10.5194/amt-8-3867-2015, 2015.